Clinical Radiology 74 (2019) 899.e1–899.e6

Contents lists available at ScienceDirect

Clinical Radiology

journal homepage: www.clinicalradiologyonline.net

DTI of great occipital nerve neuropathy: an initial study in patients with cervicogenic headache

L. Wang [a,b], S. Das [c], H. Yang [b,*]

[a] Department of Radiology, West China School of Public Health and West China Fourth Hospital, Sichuan University, Chengdu, 610041, China
[b] Department of Radiology, Affiliated Hospital of North Sichuan Medical College, Nanchong City, Sichuan Province, 637000, China
[c] North Sichuan Medical College, Nanchong City, Sichuan Province, 637000, China

ARTICLE INFORMATION

Article history:
Received 31 December 2018
Accepted 31 July 2019

AIM: To assess differences in bilateral great occipital nerves (GONs) in patients with unilateral cervicogenic headache (CEH) using diffusion tensor imaging (DTI).

MATERIALS AND METHODS: Twenty-three patients with unilateral CEH underwent GON magnetic resonance imaging (MRI). The clinical characteristics and fractional anisotropy (FA) and the apparent diffusion coefficient (ADC) values in bilateral GONs were determined by two observers with 7 and 3 years of experience in MRI. Three segments of GON were defined based on anatomy. The correlation of DTI measurements to the clinical characteristics and inter-/intra-observer performance were also evaluated.

RESULTS: The mean GON FA for the symptomatic side was significantly lower (0.198±0.056) than that on the other side (0.311±0.04; p=0.000). The mean GON ADC for the symptomatic side was significantly higher (0.682±0.174) than that on the other side (0.465±0.138; p=0.000). Among the three defined segments of GON, statistically significant differences of ADC values were not found at segment S3 (0.692±0.257 versus 0.557±0.230; p=0.068). There were statistically significant differences of FA and ADC values in bilateral GON of segments S1 and S2. The intraclass correlation coefficient (ICC) of intra-/interobserver statistical analysis showed excellent inter/intra-observer agreement for FA and ADC. Significant correlation was only found between the duration and ADC.

CONCLUSION: In patients with unilateral CEH, quantitative evaluation of the GON using DTI demonstrated FA decreases and ADC increases of the symptomatic side. Larger population and other occipital nerve neuropathy can be included in future research.

Introduction

Cervicogenic headache (CEH) is characterised by recurrent unilateral or bilateral headache originating from a neck disorder or a cervical spine lesion.[1] The prevalence of CEH ranges from 1% to 20% in individuals experiencing

* Guarantor and correspondent: H. Yang, Department of Radiology, Affiliated Hospital of North Sichuan Medical College, 63 Wenhua Road, Nanchong City, Sichuan Province, 637000, China. Tel.: +86-18398466059; fax: +86-0817-2222856.
E-mail address: yhf_nsmc@163.com (H. Yang).

https://doi.org/10.1016/j.crad.2019.07.025
0009-9260/

headache.[2,3] It is considered a referred pain innervated by the upper three cervical spinal nerves, including any structure innervated by these three spinal nerves, such as the muscles, the zygapophysal joint, and the intervertebral disc.[4] The great occipital nerve (GON) arises from the medial branch of the dorsal ramus of the C2 spinal nerve or the C3 dorsal ramus. From the suboccipital area, the nerve courses in an oblique trajectory between the semispinalis capitis and obliquus capitis inferior muscles. This area has been recognised as a potential location for GON injury and entrapment.[5–7] A GON block has become a common procedure in the diagnosis and treatment of CEH.[8,9]

Diffusion tensor imaging (DTI) is a non-invasive magnetic resonance imaging (MRI) technique for mapping fibre tracts in the peripheral nerve, which can provide valuable information about tissue architecture and microstructures.[10] In the nerve fibre, the diffusion of free water molecules varies in all directions of a three-dimensional space (anisotropy). Diffusion anisotropy is mainly determined by the orientation of fibre tracts. DTI has been used in entrapment peripheral neuropathies, such as carpal tunnel syndrome. Fractional anisotropy (FA) and the apparent diffusion coefficient (ADC) are widely used to evaluate nerve entrapment. FA reveals the coherence of oriented structures, such as myelinated nerve fibres. ADC is used in DTI to map the compactness of tissues and intercellular space and provide estimates independent of fibre directionality.[11,12] Studies have used DTI in MRI tractography for GON in healthy volunteers[13]; however, changes in DTI measurement in patients with CEH have rarely been reported. The distal brunch of GON is so tiny that the region of interest (ROI) can be set incorrectly, hindering the use of DTI for GON.

The present study aimed to assess patients with unilateral CEH by DTI and evaluate the differences in FA and ADC in both GONs symptomatically and asymptomatically. The hypothesis was that the GON of the affected side has a lower FA and a higher ADC than those of the unaffected side. The correlation of DTI measurements to clinical characteristics, as well as inter/intra-observer performances, were also evaluated.

Materials and methods

Patients

A total of 24 patients who underwent GON MRI examination with confirmed unilateral CEH by Sjaastad's criteria[14] were included in this retrospective study conducted from December 2016 to March 2018. The clinical characteristics of the patients included sex, age, laterality of pain, trigger point, head frequency, duration, and head intensity (visual analogue scale [VAS]). The exclusions were as follows: unable to tolerate the MRI examination, not suitable for image analysis (including lack of visualisation of GON fibre track), unable to localise the pain to one side, unable to quantify the pain of symptomatic side, previous head–neck trauma, hypertension, tumour, other kinds of headache, such as tension-type headache and cluster headache. The treatment outcomes will be evaluated in another study. This study was conducted only to assess nerve features in both sides of GON. This cross-sectional study was approved by the Institutional Review Board.

MRI examination and image analysis

Occipital MRI ranged from the external occipital protuberance to the C3/4 disc level. All bilateral GONs of the 23 qualified patients with suspected CEH, as determined by symptoms and physical examination, were enrolled. MRI was acquired using a 3 T MRI system (GE Discovery 750, GE Medical Systems, Milwaukee, WI, USA) with an eight-channel phased-array head–neck coil system. Coronal T2-weighted imaging (T2WI) CUBE (1 mm thickness, 192×192 matrix, 216×216 field of vision [FOV], 90° flip angle, 2,500 ms repetition time [TR]; 69 ms echo time [TE]) was performed to display the GON in multisection reconstruction. The GON was shown in all cases on both sides arising from the intervertebral foramina, coursing toward and distal to the occipital area. The GON has the inferior border of the oblique inferior muscle and semispinalis muscles as the boundary for three segments based on potential entrapment sites.[13,15] Segments S1, S2, and S3 were defined on the GON coursing by the proximal inferior border of the oblique inferior muscle, crossing the rectus capitis posterior major muscle, and piercing the semispinalis muscle (Fig 1a,c). A single-shot echo-planar imaging sequence was used in DTI (1.8 mm thickness, 64×100 matrix, 200×200 FOV, 90° flip angle, 8,500 ms TR, 57 ms TE, six excitations; b-value, 1,000 s/mm^2; six direction acquired voxel size, 2 mm isotropic), and axial T1WI (1.8 mm thickness, 256×256 matrix, 200×200 FOV, 9° flip angle, 6 ms TR, 2 ms TE) were performed to help locate GONs and set the ROI. GE ADW 4.4 workstation was used for post-processing. DTI metrics calculation, such as threshold, was processed at workstation (threshold noise 40–60, upper 3,500–3,800).

Two radiologists (with 7 and 3 years of experience in MRI with precise anatomical knowledge of GON) independently measured the FA and ADC of bilateral GONs on MR750. They also observed the changes in the morphology and signal intensity of GONs on T2WI CUBE. The FA and ADC of GONs were measured using the following steps: (1) reconstruct bilateral GON using T2WI CUBE and identify the segments of S1, S2, and S3; (2) find the target segment of GON on the reconstruction image and then localise the nerve on axial T1WI synchronously at GE workstation; (3) identify the GON on axial T1WI and confirm nerve visualisation at two close sections; (4) measure the FA and ADC values on superimposed morphological axial T1WI (Fig 1b) and ROI was delineated on the anatomical imaging. To exclude unrelated soft tissues, such as fat and muscle, the freehand tool at GE workstation was used for ROI placement based on the cross-section shape of GON on axial T1WI. For each patient, DTI measurements of the control group were acquired from the unaffected side, whereas measurements of the subject group were from the other side. FA and ADC were measured at two sections close to the defined three segments; the average on each segment was calculated. The

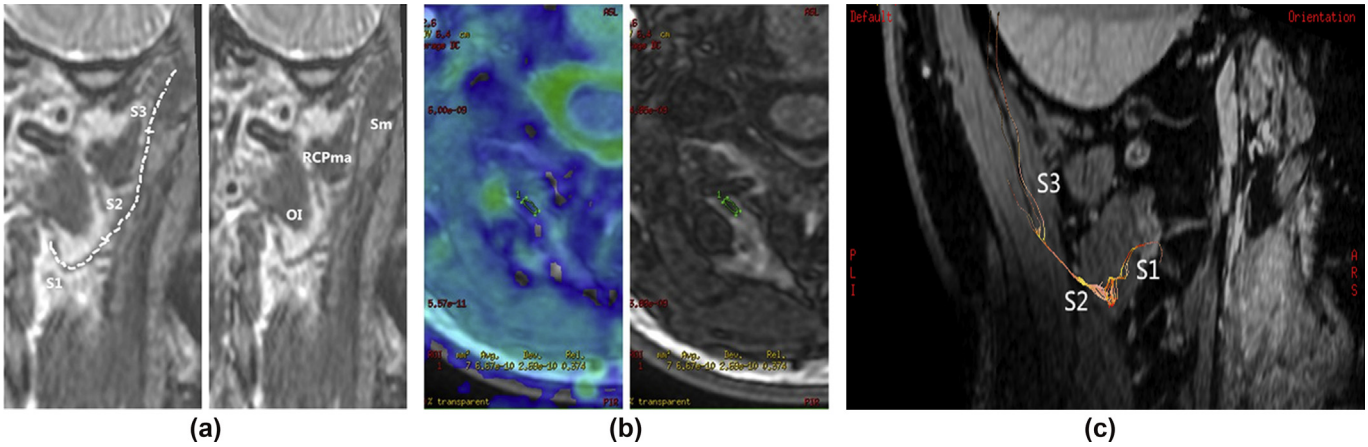

Figure 1 (a) Reconstruction CUBE of the right GON in healthy volunteer. The inferior border of the oblique inferior muscle and semispinalis muscles was defined as the boundary for the three segments (S1, S2, and S3) of the GON (OI: oblique inferior muscle, RCPma: rectus capitis posterior major muscle, Sm: semispinalis muscle). (b) Superimposed morphological axial T1WI showed ROI setting at the right GON in the same volunteer. (c) MR diffusion tensor tractography of the right GON in the same volunteer.

two radiologists were not aware of the diagnosis of the patients. Radiologist 1 obtained the first and second measurements of FA and ADC with an interval of about 1 week.

Statistical analysis

Continuous variables are presented as the mean T±SD. The independent *t*-test was employed to determine whether statistical differences existed. Inter/intra-observer performance was evaluated using the intraclass correlation coefficient (ICC): ICC>0.8 indicated excellent agreement and 0.60<ICC<0.79 indicated substantial agreement.[16] A two-tailed *p*-value of <0.05 was considered statistically significant. SPSS version 18 was used to analyse the data statistically. Moreover, the Pearson correlation coefficient was used to evaluate the correlation between the duration, headache index (HI; mean head frequency × head duration × head intensity), and DTI measurements, such as the FA and ADC of the symptomatic-side GON. The duration was determined from the onset of headache to MRI.

Results

A total of 23 patients (seven males and 16 females) with a mean age of 52.6 (range: 29–82) years were included in the study, and one female patient with lack of GON visualisation (only bilateral S1 segments were visualised on tractography) was excluded. The clinical characteristics of the 23 patients with unilateral CEH are summarised in Table 1. None of these patients were reported to have experienced head–neck trauma, hypertension, tumour, and other types of headache. All bilateral GON imaging results, including that of tractography (Fig 2), were of high quality.

The results of the quantitative analysis of the GON FA and ADC are summarised in Table 2. The mean GON FA on the symptomatic side was significantly lower (0.198±0.056) than that on the other side (0.311±0.040, p=0.000). The mean GON ADC on the symptomatic side was significantly higher (0.682±0.174) than that on the other side (0.465±0.138, p=0.000). Among the three defined segments of the GON on the symptomatic and asymptomatic sides, no significant differences in ADC were found at the site of segment S3 (0.692±0.257 versus 0.557±0.230, p=0.068). There were statistically significant differences of FA and ADC values in bilateral GONs of segments S1 and S2.

Intra/interobserver statistical analysis showed excellent agreement of the interobserver and intra-observer performances (with ICCs of 0.846–0.969 and 0.883–0.932, respectively) in FA. The interobserver performance with ICCs of 0.854–0.973 and the intra-observer performance with ICCs of 0.901–0.963 also exhibited excellent agreement in ADC (Table 3). Significant correlation between duration and ADC (Pearson correlation coefficient −0.433, p=0.039; Fig 3) was determined. Meanwhile, no significant correlation was indicated in FA versus HI, FA versus duration, and ADC versus HI (Table 4).

Table 1
The clinic characteristics of patients with unilateral CEH.

Total	23
Female	16
Male	7
Age (range)	52.61±14.29 (29–82)
Headache index	964.26±757.19
Headache frequency (days/month)	20.08±5.10
Duration of headache (weeks)	150.35±154.62
Headache duration (h/day)	6.70±3.57
Headache intensity (VAS)	6.30±1.46
Headache laterality	
Left	8
Right	15
Trigger point	
Left	7
Right	11
Both	4
None	1

VAS, visual analogue scale.

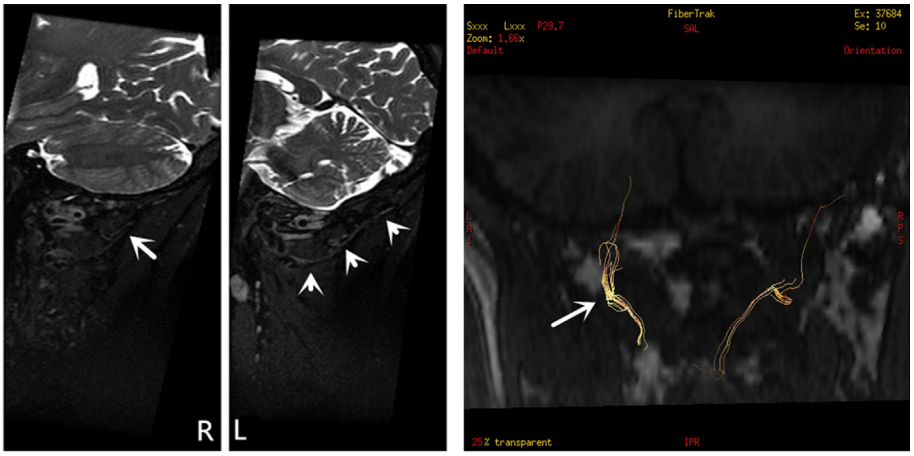

Figure 2 (a) Fat suppression CUBE T2WI of the right GON in a 49-year-old man. The left CEH is more thickened and hyperintense (arrowhead) than the right side (arrow). (b) MR diffusion tensor tractography of the same patient shows thickness and rarefaction of the left GON, especially segments S1 and S2 (arrow).

Table 2
The results of the quantitative analysis of the GON FA and ADC.

	Symptomatic side FA	Asymptomatic side FA	*p*-Value (t)	Symptomatic side ADC	Asymptomatic side ADC	*p*-Value (t)
GON	0.198±0.056	0.311±0.040	0.000 (7.905)	0.682±0.174	0.465±0.138	0.000 (4.686)
S1	0.202±0.056	0.328±0.057	0.000 (7.578)	0.664±0.280	0.418±0.127	0.001 (3.847)
S2	0.197±0.066	0.312±0.033	0.000 (7.440)	0.689±0.163	0.418±0.138	0.000 (6.093)
S3	0.196±0.062	0.294±0.063	0.000 (5.281)	0.692±0.257	0.557±0.230	0.068 (1.871)

GON, great occipital nerve; FA, fractional anisotropy; ADC, apparent diffusion coefficient.

Discussion

Diagnosing CEH presents a challenge because of the series of symptoms; in addition, CEH is often difficult to manage. In accordance with the criteria set by the International Headache Society in 2004,[17] CEH diagnosis should be supported by radiography, computed tomography (CT), or MRI; however, the relation between neck disorders and CEH has yet to be determined. Diagnostic injection of the symptomatic-side GON is considered standard. Evidence of GON entrapment and neuropathy of chronic CEH has been noted; regardless, aetiologies of uncertain original remain. This study proposes the use of non-invasive DTI to access the GON in patients with CEH.

Table 3
Interobserver and intra-observer performance in each segment of GON.

	Segment		
	S1	S2	S3
FA			
OB1 versus OB2	0.969	0.846	0.900
OB1 versus OB01	0.932	0.883	0.902
ADC			
OB1 versus OB2	0.973	0.854	0.942
OB1 versus OB01	0.963	0.901	0.923

GON, great occipital nerve; FA, fractional anisotropy; ADC, apparent diffusion coefficient.

In this study, significant differences in DTI measurements of GON FA and ADC were observed in part of the three segments, which were lower and higher on the symptomatic side, respectively. FA decreases and ADC

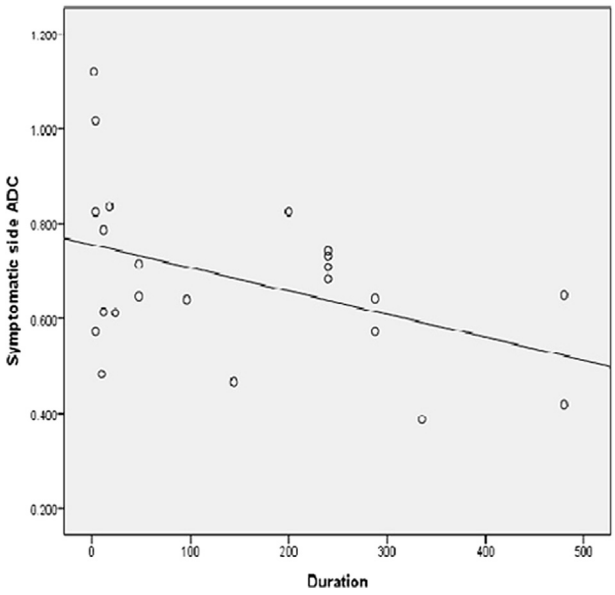

Figure 3 Pearson's correlation coefficient of the symptomatic side ADC and duration showing significant negative correlation (Pearson correlation coefficient −0.433, p=0.039).

Table 4
The correlation of the duration, headache index (HI), and diffusion tensor imaging (DTI) measurements of symptomatic side GON.

	Pearson correlation	*p*-Value
GON FA versus HI	-0.262	0.227
GON FA versus duration	-0.189	0.389
GON ADC versus HI	-0.086	0.696
GON ADC versus duration	-0.433	0.039

GON, great occipital nerve; FA, fractional anisotropy; ADC, apparent diffusion coefficient.

increases when peripheral nerves are entrapped or in other neuropathies, such as carpal tunnel syndrome, cervical disc herniation, and degenerative lumbar disorders.[12,18,19] Wallerian degeneration, intra-fascicular oedema, endoneural and epineural swelling, and perineural connective tissue thickening and fibrosis lead to the enlargement of the extracellular matrix and increase the distance between axons and nerve fascicles; thereby decreasing FA because of an isotropic situation. Intraneural oedema, axon swelling, myelinolysis, dilated intercellular space, and increased diffusion of water molecules result in a high ADC.[12,20] No significant difference in ADC was found at the site of segment S3. The distal GON was not entrapped, piercing the semispinalis muscle. The differences in FA and ADC among the three segments on the symptomatic-side GON were not compared because DTI measurements might be affected when the proximal GON was entrapped. An objective examination of the GON lesion can potentially guide treatment and improve outcomes. Current treatment based on clinical history and physical examination includes nerve block and physical treatment, such as massage. Demonstration of a normal or pathological nerve by DTI can facilitate the selection of the most suitable treatment plan for an individual who does not respond to the injections.

In the present study, coronal T2WI CUBE was performed to display the GON in multisection reconstruction to describe changes in signal, instead of a quantitative analysis. Coronal T2WI CUBE is an isotropic sequence that can acquire high soft-tissue contrast with a high signal-to-noise ratio (SNR) and high resolution in multisection reconstruction. Thus, this sequence was mainly used to assist in setting the ROI on the superimposed morphological axial T1WI. Hwang *et al.*[21] performed magnetic resonance neurography to compare nerves changes, such as the signal intensity, diameters, SNRs, and contrast-to-noise ratios of both symptomatic and asymptomatic side GONs in CEH. They found that all of these measurements were higher on the symptomatic side; however, they focused on the changes in unilateral GON as a whole, without considering the site of potential entrapment, and included patients with CEH who underwent perineural injection, radiofrequency ablation, and surgical procedures before MRI. Three segments of the GON were identified based on the anatomical structure of the potential location for nerve entrapment and the ROI was set with multisection reconstruction to evaluate changes in FA and ADC at the different sites of both GONs. The excellent ICCs of the intra/interobserver performances demonstrated the reliability of DTI measurements at different sites of bilateral GONs. CEH patients who had undergone previous treatment were not included in the study to avoid influencing the DTI measurements, although the observers were blinded to the laterality of headache.

The correlation between HI and DTI measurements was also evaluated using Pearson's correlation coefficient, and a significant negative correlation was found in ADC and duration on the symptomatic side. This result was similar to that of Hwang *et al.*[21] The result was associated with the complexity between the CEH mechanism and GON neuropathy. Kastler *et al.*[13] performed GON tractography using T1WI using the "whole-neck" streamlined approach in healthy volunteers. They acquired 32 directions to avoid problems in the uniformity of the DWI gradient directions and to meet the SNR requirement with a scanning duration of 15 minutes. Six DTI directions with NEX 6 were used to ensure an acceptable SNR and a shorter scanning duration of 6 minutes.

The present study has several limitations. First, the population of the study was small. The observers were blinded to the laterality of headache with substantial to excellent agreement of ICCs, rendering the investigation reliable. Second, changes in GON after GON injection were not evaluated, which is the subject of another study. Last, other related occipital nerves, such as the lesser occipital nerve and the third occipital nerve, were not considered. Nerve changes on DTI require further study.

In conclusion, in patients with unilateral CEH, quantitative evaluation of the GONs using DTI demonstrated FA decreases and ADC increases of the symptomatic side; however, further studies with larger sample sizes are warranted to explore the full potential of DTI for non-invasive imaging of the GONs and other occipital nerves in clinical settings.

Conflicts of interest

The authors declare no conflict of interest.

References

1. Knackstedt H, Kråkenes J, Bansevicius D, *et al*. Magnetic resonance imaging of craniovertebral structures: clinical significance in cervicogenic headaches. *J Headache Pain* 2012 Jan;**13**(1):39–44. PMID: 21947945.
2. Chaibi A, Knackstedt H, Tuchin PJ, *et al*. Chiropractic spinal manipulative therapy for cervicogenic headache: a single-blinded, placebo, randomized controlled trial. *BMC Res Notes* 2017 Jul 24;**10**(1):310. PMID: 28738895.
3. Dunning JR, Butts R, Mourad F, *et al*. Upper cervical and upper thoracic manipulation versus mobilization and exercise in patients with cervicogenic headache: a multi-center randomized clinical trial. *BMC Musculoskelet Disord* 2016 Feb 6;**17**:64. PMID: 26852024.
4. Wang E, Wang D. Treatment of cervicogenic headache with cervical epidural steroid injection. *Curr Pain Headache Rep* 2014 Sep;**18**(9):442. PMID: 25091129.
5. Pingree MJ, Sole JS, O' Brien TG, *et al*. Clinical efficacy of an ultrasound-guided greater occipital nerve block at the level of C2. *Reg Anesth Pain Med* 2017 Jan/Feb;**42**(1):99–104. PMID: 27811528.
6. Na SH, Kim TW, Oh SY, *et al*. Ultrasonic Doppler flowmeter-guided occipital nerve block. *Korean J Anesthesiol* 2010 Dec;**59**(6):394–7. PMID: 21253376.

7. Zipfel J, Kastler A, Tatu L, *et al*. Ultrasound-guided intermediate site greater occipital nerve infiltration: a technical feasibility study. *Pain Phys* 2016 Sep-Oct;**19**(7):E1027–34. PMID: 27676673.
8. Shim JH, Ko SY, Bang MR, *et al*. Ultrasound-guided greater occipital nerve block for patients with occipital headache and short term follow up. *Korean J Anesthesiol* 2011 Jul;**61**(1):50–4. PMID: 21860751.
9. Kastler A, Onana Y, Comte A, *et al*. A simplified CT-guided approach for greater occipital nerve infiltration in the management of occipital neuralgia. *Eur Radiol* 2015 Aug;**25**(8):2512–8. PMID: 25680724.
10. Brienza M, Pujia F, Colaiacomo MC, *et al*. 3T diffusion tensor imaging and electroneurography of peripheral nerve: a morphofunctional analysis in carpal tunnel syndrome. *J Neuroradiol* 2014 May;**41**(2):124–30. PMID: 23870213.
11. Naraghi A, da Gama Lobo L, Menezes R, *et al*. Diffusion tensor imaging of the median nerve before and after carpal tunnel release in patients with carpal tunnel syndrome: feasibility study. *Skeletal Radiol* 2013 Oct;**42**(10):1403–12. PMID: 23842572.
12. Wang H, Ma J, Zhao L, *et al*. Utility of MRI diffusion tensor imaging in carpal tunnel syndrome: a meta-analysis. *Med Sci Monit* 2016 Mar 4;**22**:736–42. PMID: 26942911.
13. Kastler A, Attye A, Heck O, *et al*. Greater occipital nerve MR tractography: feasibility and anatomical considerations. *J Neuroradiol* 2018 Feb;**45**(1):54–8. PMID: 28964923.
14. Sjaastad O, Saunte C, Hovdal H, *et al*. "Cervicogenic headache": an hypothesis. *Cephalalgia* 1983;**3**:249–56. PMID: 6640659.
15. Cesmebasi A, Muhleman MA, Hulsberg P, *et al*. Occipital neuralgia: anatomic considerations. *Clin Anat* 2015 Jan;**28**(1):101–8. PMID: 25244129.
16. Das SK, Yang DJ, Wang JL, *et al*. Non-Gaussian diffusion imaging for malignant and benign pulmonary nodule differentiation: a preliminary study. *Acta Radiol* 2017 Jan;**58**(1):19–26. PMID: 27055919.
17. Headache Classification Subcommittee of the International Headache Society. The international classification of headache disorders: 2nd edition. *Cephalalgia* 2004;**24**:9–160. PMID: 14979299.
18. Oikawa Y, Eguchi Y, Inoue G, *et al*. Diffusion tensor imaging of lumbar spinal nerve in subjects with degenerative lumbar disorders. *Magn Reson Imaging* 2015 Oct;**33**(8):956–61. PMID: 25979227.
19. Chen YY, Lin XF, Zhang F, *et al*. Diffusion tensor imaging of symptomatic nerve roots in patients with cervical disc herniation. *Acad Radiol* 2014 Mar;**21**(3):338–44. PMID: 24361075.
20. Zhang J, Zhang F, Xiao F, *et al*. Quantitative evaluation of the compressed L5 and S1 nerve roots in unilateral lumbar disc herniation by using diffusion tensor imaging. *Clin Neuroradiol* 2017 Aug 21. PMID: 28828579.
21. Hwang L, Dessouky R, Xi Y, *et al*. MR neurography of greater occipital nerve neuropathy: initial experience in patients with migraine. *AJNR Am J Neuroradiol* 2017 Nov;**38**(11):2203–9. PMID: 28882864.